



Li₂SrSi₂N₄:Eu²⁺: Electronic structure and luminescence of a red phosphor

Quansheng Wu^{a,b,*}, Yanyan Li^c, Chuang Wang^d, Jiangshui Luo^{a,b,*}

^a Collaborative Innovation Center of Clean Energy, Longyan University, Longyan 364000, Fujian, China

^b Fujian Provincial Key Laboratory of Clean Energy Materials, College of Chemistry and Materials Science, Longyan University, Longyan 364000, Fujian, China

^c Institute of Physics and Optoelectronics Technology, Baoji University of Arts and Sciences, Baoji 721016, China

^d College of New Energy, Bohai University, Jinzhou 121000, China

ARTICLE INFO

Keywords:

Li₂SrSi₂N₄:Eu²⁺
Red phosphor
Nitridosilicates
Photoluminescence
LED

ABSTRACT

Rare earth doped lithium containing nitridosilicates have become a hot spot in phosphors research because of their excellent luminescent properties. Here, the nitridolithosilicate Li₂SrSi₂N₄:Eu²⁺ was successfully synthesized by solid-state reaction. Li₂SrSi₂N₄:Eu²⁺ shows a red emission at 615 nm with an FWHM = 100 nm at the excitation of the near ultraviolet spectral region. Rietveld refinement on the powder XRD pattern revealed that Li₂SrSi₂N₄ crystallizes in the cubic space group Pa $\bar{3}$ (no. 205) [Z = 12, a = 10.7242(3) Å, V = 1233.37(9) Å³] and exhibits a three-dimensional network with solely vertex-sharing [SiN₄] tetrahedral. The electronic structure of Li₂SrSi₂N₄ was explored using density functional theory (DFT) methods. The results show that Li₂SrSi₂N₄:Eu²⁺ can benefit the development of the novel red luminophor.

1. Introduction

With the shortage of fossil energy and the increasingly serious climate problems, people pay more and more attention to energy efficiency issue. It is well known that a large amount of energy is used for lighting and display, so people have been looking for more efficient, energy-efficient, and environmentally friendly light sources. White light-emitting diodes (WLEDs) as a new type of solid light source, with high efficiency, energy saving, environmental protection, stable and durable, etc., and gradually replace incandescent and fluorescent lamps, become the next generation of new solid-state lighting source. At present, the mainstream way to obtain WLEDs is phosphor conversion technology: the phosphor powder coating on the LED chip, using LED chip to activate phosphor powder and then combining to achieve white light emission [1–7]. Therefore, phosphors play a decisive role in luminous performance of WLEDs (such as luminous efficiency, color temperature, etc.) In addition, the red phosphor powder is not only effective in improving the color index of WLEDs, but also greatly improves the luminous efficiency of WLEDs by controlling the distribution of emission spectra. Therefore, the research and development of red phosphors can meet the important demand of luminescent materials in practical application.

In recent years, lithium containing nitrides (M-Li/Mg-Si/Al-N, M = Ca, Sr, Ba) have become the research focus of luminescent materials for WLED because of their narrow band red emission properties, such as Sr [LiAl₃N₄]:Eu²⁺ [8], CaLiAl₃N₄:Eu²⁺ [9], Ca₂[Li₂Mg₂Si₂N₆]:Eu²⁺ [10],

Ca_{1.75}[Li_{10.5}Al₃₉N₅₅]:Eu²⁺ [11], Ca₃[Li₂MgSi₂N₆]:Eu²⁺ [12]. Thereinto, Sr[LiAl₃N₄]:Eu²⁺, as a representative of its narrow band red emission, high quantum efficiency and excellent thermal stability, has great potential for practical application for WLEDs. For lithium containing nitrides, the network is made up of corner- and edge-sharing Li (Mg)N₄ tetrahedra and Si(Al)N₄ tetrahedra and the M (M = Li, Ca, Sr, Ba) cations occupy the interstitial spaces between the nitridometallate framework of Si/AlN₄ tetrahedra [4,8]. When the rare earth ions Eu²⁺ substitutes M, Eu²⁺ will be in a special rigid structure. Narrow band red light emission can be achieved due to the confinement of the local structure and the strong covalent bonding of the nitride [13]. The results show that lithium containing nitrides are one of the potential substrates for use as Eu²⁺ doped red-emitting phosphors.

This research builds on the work of Zeuner et al. [14], describing the nitridolithosilicate Li₂SrSi₂N₄. In this contribution, the preparation and structural features of Li₂SrSi₂N₄:Eu²⁺ phosphors are reported. The band structure and photoluminescence properties of Eu²⁺ activated Li₂SrSi₂N₄ have been studied in detail for the first time. The Eu²⁺ activated Li₂SrSi₂N₄ exhibited red emission under the excitation of near ultraviolet light. We also investigated the morphology and the thermal quenching property of Li₂SrSi₂N₄:Eu²⁺.

* Corresponding authors at: Collaborative Innovation Center of Clean Energy, Longyan University, Longyan 364000, Fujian, China.
E-mail addresses: wqs@lyun.edu.cn (Q. Wu), proticils@gmail.com (J. Luo).

2. Experiment section

2.1. Synthesis

The synthesis of $\text{Li}_2\text{Sr}_{1-x}\text{Si}_2\text{N}_4:x\text{Eu}^{2+}$ ($x = 0\text{--}0.03$) was achieved by conventional solid-state method using Li_3N (Aldrich, > 99.50%), Si_3N_4 (Aldrich, 99.50%), Sr_3N_2 (Aldrich, > 99.50%), and EuCl_3 (Aldrich, 99.999%) as raw materials. All operations are carried out in N_2 -filled glove boxes (Mikrouna, Super (1220/750/900), $\text{N}_2 > 99.9995\%$, $\text{H}_2\text{O} < 1$ ppm, $\text{O}_2 < 1$ ppm). The raw materials were thoroughly mixed in stoichiometric proportion in an agate mortar. The powder mixture was subsequently filled into a small cylindrical Al_2O_3 crucible (diameter of 9 mm) and compacted, and then rapidly heated ($15^\circ\text{C min}^{-1}$) to 900°C within 3 h in a horizontal tube furnace. The furnace need to vacuum before heating, then pass into forming gas atmosphere ($\text{N}_2:\text{H}_2 = 95:5$). The sintered samples strip off the surface oxidation section and then ground the remaining parts into powder. The powders of $\text{Li}_2\text{SrSi}_2\text{N}_4:\text{Eu}^{2+}$ are stable in the air and water, and there is no decomposition and color change in the air and water contact for several days.

2.2. Characterization

2.2.1. Powder X-ray diffraction (XRD)

Powder diffraction data were collected on a Bruker D2 PHASER X-ray Diffractometer (Cu-K α 1 radiation, graphite monochromator) at an accelerating voltage of 30 kV. The data acquisition was performed in the range of $10\text{--}100^\circ$ with 0.03° per step. Rietveld refinement on the powder XRD pattern was carried out using the general structure analysis system (GSAS) [15].

2.2.2. Electronic Structure calculations

The electronic structure of $\text{Li}_2\text{SrSi}_2\text{N}_4$ was calculated using density functional theory (DFT) methods [16–19] performed with the Cambridge Sequential Total Energy Package (CASTEP) code on the basis of the single crystal structure of $\text{Li}_2\text{SrSi}_2\text{N}_4$. The source of this crystal structure was reported by Zeuner [14]. The local-density approximations based on density functional theory were chosen for the theoretical basis of the density function.

2.2.3. Ultraviolet-visible (UV/vis) Spectroscopy

The diffuse reflectance UV–vis absorption spectra were measured using a Perkin-Elmer 950 spectrometer, whereas BaSO_4 was used as a reference.

2.2.4. Luminescence

An FLS-920T fluorescence spectrophotometer equipped with a 450 W xenon lamp and an F900 nanosecond flash hydrogen lamp was used for recording the photoluminescence spectra and decay curves, respectively. The thermal quenching performance was determined using a cartridge heater and a TAP-02 high temperature fluorescence controller which were attached to the FLS-920T fluorescence spectrophotometer.

2.2.5. Powders morphology

For powders morphology measurements, a scanning electron microscopy (SEM; S-3400, Hitachi, Japan) and a transmission electron microscopy (TEM, FEI Tecnai F30) were used. The TEM equipped with an energy-dispersive X-ray (EDX) detector for elemental analysis was employed.

2.2.6. Fabrication of WLEDs

A SH2012 ultrasonic wire welding machine was used to the fabrication of WLEDs device. The electroluminescent spectrum of the LED package was measured by a PMS-80 UV–vis–near IR spectrophotometer.

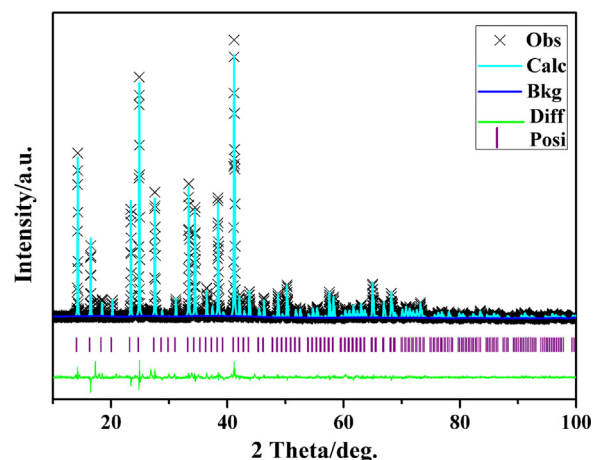


Fig. 1. Rietveld refinement of $\text{Li}_2\text{SrSi}_2\text{N}_4$. Observed (crosses), calculated (blue line), difference profile (green line) and Bragg positions (purple vertical bars). (For interpretation of the references to color in this figure legend, the reader is referred to the web version of this article.)

3. Results and discussion

3.1. Phase identification and morphology observation

In order to confirm the structure and phase purity of the as-prepared $\text{Li}_2\text{SrSi}_2\text{N}_4$ sample, the Rietveld refinement of $\text{Li}_2\text{SrSi}_2\text{N}_4$ was performed based on the single crystal data reported by Zeuner [14]. As exhibited in Fig. 1, the observed XRD profiles match well with the calculated profiles and the values of reliability factors are low ($R_p = 8.26\%$, $R_w p = 6.34\%$, and $\chi^2 = 1.38$). The crystallographic information for $\text{Li}_2\text{SrSi}_2\text{N}_4$ obtained from Rietveld refinement is summarized in Table 1. $\text{Li}_2\text{SrSi}_2\text{N}_4$ crystallizes in the cubic space group $\text{Pa}\bar{3}$ (no. 205) [$Z = 12$, $a = 10.7242(3)$ Å, $V = 1233.37(9)$ Å 3] and exhibits a three-dimensional network with solely vertex-sharing [SiN $_4$] tetrahedra, as shown in Fig. 2a. A siebener rings (Net39) can be found in the cubic unit cells which consist of 24 [SiN $_4$] tetrahedral connected by vertex-sharing. Sr^{2+} and Li^+ occupy the channel of Si–N network to charge compensate the anionic framework. As displayed in Fig. 2b, Sr^{2+} occupies two independent crystallographically sites and is coordinated by the six N atoms in a highly symmetric surrounding. Sr1 shows trigonal prism coordination with Sr–N distances ranging from 2.68 to 2.69 Å and Sr2 shows trigonal antiprism coordination with Sr–N distances of 2.76 Å. The Sr–N distances correspond well with other known lithium strontium nitrides such as $\text{Sr}[\text{LiAl}_3\text{N}_4]$ [2.69–2.91 Å] [8] or $\text{Li}_4\text{Sr}_3\text{Si}_2\text{N}_6$ [2.62–3.28 Å] [20].

The serial XRD patterns of $\text{Li}_2\text{Sr}_{1-x}\text{Si}_2\text{N}_4:x\text{Eu}^{2+}$ ($x = 0.005\text{--}0.03$) are shown in Fig. 3. With Eu^{2+} incorporating, the XRD profiles of the samples retain a good single phase without any impurity phase. Moreover, there is no shift of the diffraction peaks with Eu^{2+} doping. It is well known that Eu^{2+} and Sr^{2+} have similar radii (Eu^{2+} : 1.31 Å, CN = 6; Sr^{2+} : 1.32 Å, CN = 6) [21] and the same form charge. When Eu^{2+} was incorporated in the lattice, it will occupy the position of Sr^{2+} to reduce the lattice distortion energy, and the host lattice is almost unchanged. So the diffraction peaks do not shift with Eu^{2+} doping.

It is well known that the luminescence performance of phosphors for WLEDs is closely related to the microstructure of the phosphor powder. The micrographs of the microstructure of $\text{Li}_2\text{Sr}_{1-x}\text{Si}_2\text{N}_4:x\text{Eu}^{2+}$ ($x = 0, 0.005$) are investigated, as shown in Fig. 4a–b. As seen, the particles exhibit an irregular-shaped morphology with smooth surface and compact edges. Moreover, the powder has good dispersion and exhibits a narrow particle size distribution with a diameter of about 2–6 μm . The fine structure observations of the $\text{Li}_2\text{SrSi}_2\text{N}_4$ were carried out by HRTEM techniques, as shown in Fig. 4c–d. The HRTEM image in Fig. 4d corresponds to the selected area in Fig. 4c. The d-spacing of

Download English Version:

<https://daneshyari.com/en/article/7840065>

Download Persian Version:

<https://daneshyari.com/article/7840065>

[Daneshyari.com](https://daneshyari.com)